

Precision measurement of the K_S meson lifetime with the KLOE detector

The KLOE Collaboration

F. Ambrosino^{3,4}, A. Antonelli¹, M. Antonelli^{1,a}, F. Archilli^{8,9}, G. Bencivenni¹, C. Bini^{6,7}, C. Bloise¹, S. Bocchetta^{10,11}, F. Bossi¹, P. Branchini¹¹, G. Capon¹, T. Capussela¹, F. Ceradini^{10,11}, P. Ciambrone¹, A. De Angelis¹⁴, E. De Lucia¹, M. De Maria¹⁵, A. De Santis^{6,7}, P. De Simone¹, G. De Zorzi^{6,7}, A. Denig², A. Di Domenico^{6,7}, C. Di Donato⁴, B. Di Micco^{10,11}, M. Dreucci^{1,b}, G. Felici¹, S. Fiore^{6,7}, P. Franzini^{6,7}, C. Gatti¹, P. Gauzzi^{6,7}, S. Giovannella¹, E. Graziani¹¹, M. Jacewicz¹, V. Kulikov¹³, J. Lee-Franzini^{1,12}, M. Martini^{1,5,16}, P. Massarotti^{3,4}, S. Meola^{3,4}, S. Miscetti¹, M. Moulson¹, S. Müller², F. Murtas¹, M. Napolitano^{3,4}, F. Nguyen^{10,11}, M. Palutan¹, A. Passeri¹¹, V. Patera^{1,5}, P. Santangelo¹, B. Sciascia¹, A. Sibidanov¹, T. Spadaro¹, C. Taccini^{10,11}, L. Tortora¹¹, P. Valente⁷, G. Venanzoni¹, R. Versaci^{1,5,17}

¹Laboratori Nazionali di Frascati dell'INFN, Frascati, Italy

²Institut für Kernphysik, Johannes Gutenberg—Universität Mainz, Mainz, Germany

³Dipartimento di Scienze Fisiche dell'Università "Federico II", Napoli, Italy

⁴INFN Sezione di Napoli, Napoli, Italy

⁵Dipartimento di Energetica dell'Università "La Sapienza", Roma, Italy

⁶Dipartimento di Fisica dell'Università "La Sapienza", Roma, Italy

⁷INFN Sezione di Roma, Roma, Italy

⁸Dipartimento di Fisica dell'Università "Tor Vergata", Roma, Italy

⁹INFN Sezione di Roma Tor Vergata, Roma, Italy

¹⁰Dipartimento di Fisica dell'Università Roma Tre, Roma, Italy

¹¹INFN Sezione di Roma Tre, Roma, Italy

¹²Physics Department, State University of New York, Stony Brook, USA

¹³Institute for Theoretical and Experimental Physics, Moscow, Russia

¹⁴Università di Udine and LIP/IST, INFN Sezione di Trieste, Trieste, Italy

¹⁵Università di Udine and IUAV, Venezia, Italy

¹⁶Present address: Dipartimento di Scienza e Tecnologie applicate, Università Guglielmo Marconi, Roma, Italy

¹⁷Present address: CERN, 1211 Geneva 23, Switzerland

Received: 11 November 2010 / Revised: 11 February 2011 / Published online: 24 March 2011
© The Author(s) 2011. This article is published with open access at Springerlink.com

Abstract Using a large sample of pure, slow, short lived K^0 mesons collected with KLOE detector at DAΦNE, we have measured the K_S lifetime. From a fit to the proper time distribution we find $\tau(K_S) = (89.562 \pm 0.029_{\text{stat}} \pm 0.043_{\text{sys}})$ ps. This is the most precise measurement to date of the short lived K^0 meson lifetime, in good agreement with the world average derived from previous measurements. We observe no dependence of the lifetime on the direction of the K_S in galactic coordinates.

1 Introduction

We have collected very large samples, $\mathcal{O}(10^9)$ events), of slow K -mesons of well known momentum, with the KLOE detector at DAΦNE. Kaons originate from the decay of ϕ -mesons produced in e^+e^- collisions. We have used the above samples to measure many properties of kaons such as masses, branching ratios and lifetimes, Refs. [1–10]. The ultimate motivation was the determination of the quark mixing parameter V_{us} , see Ref. [7]. KLOE had not however attempted to measure the K_S lifetime. From the reaction chain $e^+e^- \rightarrow \phi$, $\phi \rightarrow K_L K_S$ (K_L is unobserved) and $K_S \rightarrow \pi^+\pi^-$ decay, we determine the K_S -meson vector momentum p_K , the kaon production point P and its decay point D. From our best estimate of p_K , P and D, defined in detail later, we obtain the decay proper time of the K_S .

^ae-mail: Mario.Antonelli@lnf.infn.it

^be-mail: Marco.Dreucci@lnf.infn.it

A fit to the proper time distribution gives the K_S -meson lifetime. The vast available statistics allows us to select some 20 million $K_S \rightarrow \pi^+\pi^-$ decays with favorable configuration to provide the most accurate and least biased measurement of time. Averaging over the sample gives a statistical accuracy of $\sim 2 \mu\text{m}$ in the measurement of the kaon mean decay length.

The KLOE detector energy scale calibration is based on the value of the ϕ -meson mass, $M(\phi) = 1019.455 \pm 0.020 \text{ MeV}$, Ref. [8], from the observation of the $g - 2$ depolarizing resonances at Novosibirsk. Thus the KLOE energy/momentum scale accuracy is $\sim 0.002\%$. In addition KLOE fully accounts for radiative corrections, which are crucial in obtaining final accuracies well below 0.1% for any measured physical quantity. Radiative corrections are incorporated in the KLOE Monte Carlo Geanfi, see Ref. [9], at the event generator level. Thus the MC generated events are fully dressed of the appropriate radiation, both initial and final. Our measurement of the neutral kaon mass fully exploited the above feature, Ref. [10]. In the following we use our value of the kaon mass, $M_K = (497.583 \pm 0.021) \text{ MeV}$.

The KLOE detector has been described in all the references mentioned above, see also Refs. [11–14]. In particular Ref. [7] summarizes the use of the KLOE detector in collecting kaon data and reconstructing all decay channels.

2 Data reduction

Data used in this analysis, corresponding to an e^+e^- integrated luminosity of 0.4 fb^{-1} , were collected in 2004 with the KLOE detector at DAΦNE, the Frascati ϕ -factory. DAΦNE is an e^+e^- collider operating at a center of mass energy $\sqrt{s} \sim 1020 \text{ MeV}$, the ϕ -meson mass. Beams collide at an angle of $\pi - 0.025 \text{ rad}$. For each run of about 2 hours, we measure the CM energy \sqrt{s} , \mathbf{p}_ϕ (about 13 MeV in the horizontal plane) and the average position of the beams interaction point P using Bhabha scattering events. Data are combined into 34 run periods, each corresponding to an integrated luminosity of about 15 pb^{-1} . For each run set, we generate a sample of Monte Carlo (MC) events of three times equivalent statistics [9]. We use a coordinate system with the z -axis along the bisector of the external angle of the e^+e^- beams, the so called beam axis, the y -axis pointing upwards and the x -axis toward the collider center.

$K_S \rightarrow \pi^+\pi^-$ decays are reconstructed from two opposite sign tracks which must intersect at a point D with $r_D < 10 \text{ cm}$ and $|z_D| < 20 \text{ cm}$, where $x = y = z = 0$ is the average e^+e^- collision point. The invariant mass of the two tracks, assumed to be pions, must satisfy $|M_{\pi\pi} - M_{K^0}| < 5 \text{ MeV}$. D is taken as the decay point. The kaon momentum \mathbf{p}_K can be obtained from the sum of the pion momenta. Since \mathbf{p}_ϕ is well known, the magnitude of the kaon momentum can be also obtained from the knowledge of the kaon

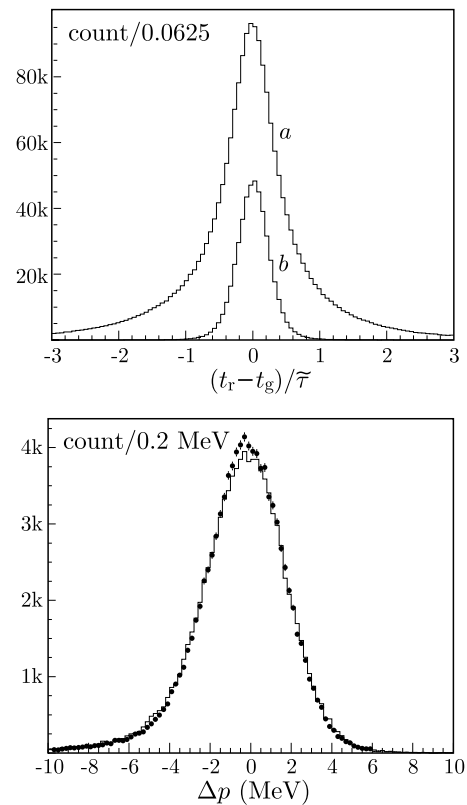


Fig. 1 *Top.* Monte Carlo. Reconstructed minus generated time, $t_r - t_g$, distribution for the initial K_S sample (rms spread $\sim 0.86\tilde{\tau}$), histogram *a* and after cuts and geometrical fit, *b*, (rms spread $\sim 0.32\tilde{\tau}$). *Bottom.* Distribution of $\Delta p = p_K - p'_K$ for data (*dots*), and Monte Carlo (*line*) corresponding to the initial sample selection, histogram *a*, *top*. The tail at left is due to the initial state radiation

direction (always from pions) and the kinematic. We call the latter value \mathbf{p}'_K . In this analysis we use \mathbf{p}'_K to evaluate $\beta\gamma$, being less sensitive to the momentum calibration. The magnitude of the two values of the kaon momentum must agree to within 10 MeV. Figure 1 bottom shows the distribution of $\Delta p = p_K - p'_K$, the difference in magnitude of the two momentum determinations, for data and MC. If the two tracks intersect in more than one point satisfying the above requirements, the one closest to the origin is retained as the K_S decay point. We refer to the finding of D as vertexing. The above procedure selects a $K_S \rightarrow \pi^+\pi^-$ sample almost 100% pure. The largest background contribution, $K_L \rightarrow \pi^+\pi^-$ decay close to the interaction point, is smaller than 5×10^{-6} . For each event we need the kaon production point P. In fact only the z -coordinate of P is required since the interaction region is 2–3 cm long while the other dimensions are negligible and the x , y coordinates well known. P lies on the beam axis and is taken as the point of closest approach to the K_S path as determined by the $\pi^+\pi^-$ tracks. The resolution in z_P is about 2 mm. Events with $|z_P| > 2 \text{ cm}$ are rejected. From the length of PD and p'_K we compute the proper time in units of a reference value of $\tilde{\tau}$, the lifetime

value used in our MC, $\tilde{\tau} = 89.53$ ps. Its residual distribution is shown in Fig. 1 top, histogram a. The distribution has an rms spread of $0.86 \tilde{\tau}$ and is not symmetric. Time resolution can be improved discarding events with poor vertexing resolution. From MC we observe that bad vertex reconstruction is correlated with large values of Δp . Therefore we cut the angular regions where Δp begins significantly to increase. We retain events with $\cos \alpha_{\pi\pi} < -0.87$, being $\alpha_{\pi\pi}$ the opening angle of the pion pair. We must also distinguish between the two $\pi^+\pi^-$ ‘V’ configurations illustrated in Fig. 2, because they are differently affected by a miscalibration of pion momentum. Calling \mathbf{r} and \mathbf{s} the projections of kaon and positive pion on the $\{x, y\}$ plane, $\alpha_{\pi^+K}^\perp$ is defined as

$$\alpha_{\pi^+K}^\perp = \text{sign}((\mathbf{r} \times \mathbf{s})_z) \arccos\left(\frac{\mathbf{r} \cdot \mathbf{s}}{rs}\right).$$

The angle $\alpha_{\pi^+K}^\perp$ is defined in $\{-\pi, \pi\}$. Positive sign corresponds to the configuration of Fig. 2, left. Applying the cut $0.5 < |\alpha_{\pi^+K}^\perp| < 2.2$ rad we retain only events with good D vertex position resolution. Finally, we apply the cuts $|M_{\pi\pi} - M_K| < 2$ MeV and $-0.5 < \cos \theta(\pi^\pm) < +0.5$, which still contribute to improve the time resolution. All of these angles are measured in the laboratory system. After applying the cuts described above, only $\sim 1/3$ of the events survive while the rms residual time spread is reduced to $0.63 \tilde{\tau}$. Another significant improvement is obtained performing a geometrical fit of each event. We chose a new point P' on the beam axis and a new decay point D' on a line through P', parallel to \mathbf{p}_K , so as to minimize the χ^2 function

$$\frac{|\mathbf{r}_{D'} - \mathbf{r}_D|^2}{\sigma_D^2} + \frac{(z_{P'} - z_P)^2}{\sigma_z^2}.$$

The proper time residual distribution, after all cuts and the fit, is shown in Fig. 1 top, curve b. The rms spread is $0.32 \tilde{\tau}$. We check the correctness of the K_S direction using a sample of K_L -mesons reaching the calorimeter, where they are detected by nuclear interactions. The K_L interaction point in the calorimeter together with the known ϕ momentum gives an independent determination of the K_S direction. The calibration is checked comparing for each run period the difference of the two determinations. Typically for a 20k events sample we find a $\sim 0.002^\circ$ difference (corresponding to $10^{-5} \mu\text{m}$ on K_S decay length), well within the error. We found consistent determinations in all periods. The final efficiency for $K_S \rightarrow \pi^+\pi^-$ detection is shown in Fig. 3 as a function of proper time. While the $K_S \rightarrow \pi^+\pi^-$ reconstruction efficiency, about 68% due to the geometrical acceptance, does not depend on the K_S direction, the efficiency after our sample selection does. Almost flat in proper time it is on average $\sim 9\%$. Errors in the reconstruction of the pion tracks can bias the position of D. Studies of the

Fig. 2 The two configurations for a $K_S \rightarrow \pi^+\pi^-$ decay

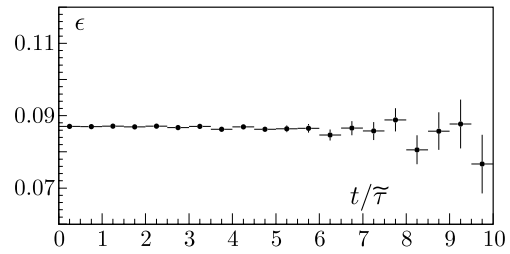
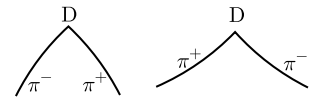


Fig. 3 Monte Carlo: final efficiency, averaged over all K_S directions, as a function of the proper time in a single run period

momentum calibration [10] show a fractional error of about 2×10^{-4} . For a ~ 200 MeV/c transverse momentum track the above error corresponds to about 0.3 mm change on the radius of the track. To check the correctness of track reconstruction we divide all data into two samples with $\alpha_{\pi^+K}^\perp > 0$ and < 0 (see Fig. 2). A track momentum overestimate (underestimate) moves the position of D toward (away from) P for $\alpha_{\pi^+K}^\perp > 0$ and viceversa for $\alpha_{\pi^+K}^\perp < 0$. The K_S lifetimes evaluated for the two samples differ by $\sim 6\%$, consistent with what expected from our momentum accuracy. We do correct for this effect. From MC–Data comparison we obtain the correction, $\Delta \ell_K$, to be applied to the K_S decay length, as a function of Δp , used as an estimator of the momentum miscalibration. After applying this correction the 6% difference mentioned above is reduced to $\sim 10^{-3}$, although the new average result is only $\sim 2\sigma$ (0.1%) different from the result before applying it.

3 Proper time distribution fit

MC and data studies show that the time resolution is well described by the sum of two Gaussians. Fit quality is poor if we try to use a simple Gaussian. The resolution function, normalized to unity, is taken as:

$$r(t, \tau, \sigma_1, \sigma_2, \alpha) = \frac{\alpha}{\sigma_1 \sqrt{2\pi}} \exp\left(-\frac{t^2}{2\sigma_1^2}\right) + \frac{1-\alpha}{\sigma_2 \sqrt{2\pi}} \exp\left(-\frac{t^2}{2\sigma_2^2}\right)$$

and the decay function, for a lifetime τ , is:

$$d(t) = \frac{1}{\tau} \times \exp\left(-\frac{t}{\tau}\right) \times \theta(t).$$

The expected decay curve, normalized to unity, is given by the convolution

$$g(t) = \int_{-\infty}^{\infty} d(\eta)r(t - \eta) d\eta.$$

Allowance must be still be made for small mistakes in the reconstruction of the decay and production position, D and P. A shift δ in the proper time is therefore introduced. Thus the function which we use for fitting the observed distribution is

$$f(t, \tau, \sigma_1, \sigma_2, \alpha, \delta) = g(t - \delta).$$

The four parameters, $\sigma_1, \sigma_2, \alpha, \delta$ in $f(t)$ depend on colatitude and azimuth, θ and ϕ , of the kaon and it is not realistic to attempt to obtain them from MC. We divide the data in a 20×18 grid in $\cos\theta, \phi$ and fit each data set for the lifetime τ with the above parameters free. We retain only events in a fiducial volume (FV) with $|\cos\theta| < 0.5$,¹ discarding in this way only $\sim 8\%$ of the events, mainly mis-reconstructed events. We therefore perform 180 independent fits only to events in a 10×18 grid. The fit range, -1 to $6.5\tilde{\tau}$, is divided in 15 proper time bins. The kaon lifetime is obtained as the weighted average of the 180 τ_i values

$$\tau(K_S) = \langle \tau \rangle = \frac{\sum_i \tau_i}{\sum_i \frac{1}{\sigma^2(\tau_i)}} / \sum_i \frac{1}{\sigma^2(\tau_i)}.$$

The corresponding χ^2 value is $\chi^2 = \sum_i (\tau_i - \langle \tau \rangle)^2 / \sigma^2(\tau_i)$. We find $\chi^2/\text{dof} = 202/179$ for a confidence level, CL, of 11.4%. The normalized residuals the 180 fit values τ_i have an rms spread of 1.1. Table 1 gives the average correlations between fit parameters and Fig. 4 top shows a fit example.

The resolution $(\sqrt{\alpha\sigma_1^2 + (1-\alpha)\sigma_2^2})$ versus $\{\theta, \phi\}$ is shown in Fig. 4 bottom. The resolution varies from $0.22\tilde{\tau}$ to $\sim 0.27\tilde{\tau}$ over the accepted $\{\cos\theta, \phi\}$ range with an average of $0.24\tilde{\tau}$. The δ_i values show a dependence on ϕ with period 2π corresponding to a shift of the position of P of $\sim -10 \mu\text{m}$ in y and $\sim 50 \mu\text{m}$ in x . In addition, a very small, 10^{-4} , eccentricity of the drift chamber is evident. All these effects are consistent with mechanical and surveying inaccuracies. When fitting MC data with the procedure described above we find a bias on the lifetime measurement, $\tilde{\tau}/\tau_{\text{fit}}^{\text{MC}} = 1.00036 \pm 0.00019$. The lifetime fit result $\langle \tau \rangle$ has been corrected for this factor and the uncertainty has been included in the final statistical error.

4 Systematic uncertainties and result

Changes in analysis cuts have been made to study the stability of the result with an increased or decreased fraction of events with poor calibration and resolution of the decay length. The values of all the cuts described in Sect. 2 have been varied for a corresponding change of $\sim \pm 60\%$ on the efficiency. The FV of the kaon polar angle has been varied from 0.3 to 0.7. The result is found to be stable within 1.5σ ,

¹The kaon angular distribution in the lab is $\sim \sin^2\theta$.

Table 1 Correlation of fit parameters (averaged values)

	σ_1	σ_2	α	δ
τ_S	0.18	0.09	0.11	0.62
σ_1		0.50	0.75	0.28
σ_2			0.69	0.11
α				0.16

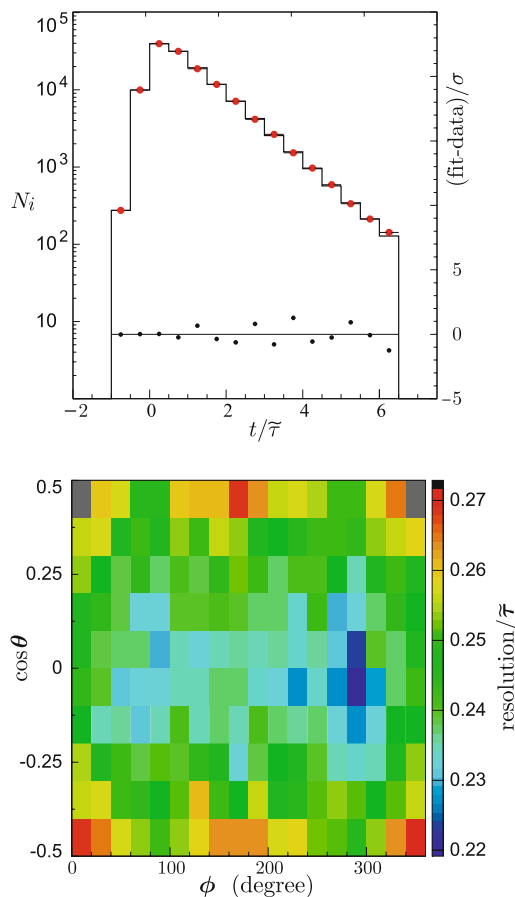


Fig. 4 Top: an example of the fit with $\chi^2/\text{dof} = 8/10$, dots are data, the line is the fit result. Bottom: proper time resolution, in units of $\tilde{\tau}$, as a function of ϕ and $\cos\theta$

(considering only the uncorrelated part of the statistical error) corresponding to a systematic uncertainty of 0.024 ps. The systematic uncertainty due to the fit range, 0.012 ps, has been evaluated including or excluding left and right bins on the tails. The lifetime variation is not consistent with the statistical fluctuation which have been expected to be very small, about 1%. The measurement of $\beta\gamma$ and the decay position are independent. The uncertainty on the calibration of p'_K , directly related to the \sqrt{s} calibration [10], gives an uncertainty of 0.033 ps. The uncertainty due to K_S mass is 0.004 ps. All fits are performed assuming uniform efficiency versus proper time, resulting in an uncertainty of 0.005 ps. Table 2 summarizes all systematic errors. The result is stable

Table 2 Systematic error contributions

Source	Absolute value (ps)
Cuts & FV	0.024
Fit range	0.012
p'_K calibration	0.033
Kaon mass	0.004
Efficiency	0.005
Total	0.043

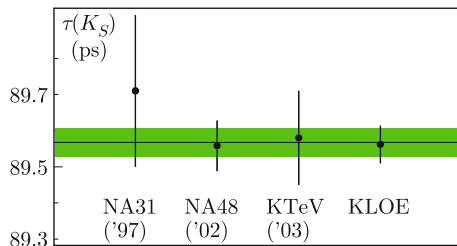


Fig. 5 Recent K_S lifetime measurements. The green band represents the new world average, $\tau(K_S) = 89.567 \pm 0.039$ ps

across the entire data taking period. Without vertex correction the result changes by ~ 2 standard deviation, but stability with the run period is lost. Our result for the K_S lifetime is:

$$\tau(K_S) = 89.562 \pm 0.029_{\text{stat}} \pm 0.043_{\text{sys}} \text{ ps.} \tag{1}$$

Subdividing the data in 9 ϕ intervals and summing over $\cos\theta$ the ϕ dependence of the lifetime becomes quite obvious. The average of the 9 $\tau(K_S)$ values are of course exactly as (1) but $\chi^2/\text{dof} = 24/8$ for a CL of $\sim 0.2\%$. Enlarging the statistical error by a factor $\sqrt{24/8}$ restores $\chi^2 = 8$ (CL = 43%) and corresponds to $\tau(K_S) = 89.562 \pm 0.050$ ps, an error very close to $\sqrt{0.029^2 + 0.043^2} = 0.052$ ps, consistent with our evaluation of the systematic uncertainties in (1).

The result of (1) is in agreement with recent measurements, Refs. [15–17], as shown in Fig. 5. Including the present measurement, the new world average for the K_S lifetime is $\tau_S = 89.567 \pm 0.039$ ps, with $\chi^2/\text{dof} = 0.5/3$, or CL $\sim 92\%$.

In KLOE we can measure the lifetime for kaons traveling in different directions. We choose three orthogonal directions, the first being $\{\ell_1, b_1\} = \{264^\circ, 48^\circ\}$ in galactic coordinates. This is the direction of the dipole anisotropy of the cosmic microwave background (CMB), Refs. [18]. The other two directions are taken as $\{\ell_2, b_2\} = \{174^\circ, 0^\circ\}$ and $\{\ell_3, b_3\} = \{264^\circ, -42^\circ\}$. After transforming the kaon momentum to the above systems, we retain only events with \mathbf{p}_K inside a cone of 30° opening angle, parallel (+) and antiparallel (–) to the chosen directions and evaluate the kaon lifetime. The 6 results are consistent with (1). Defining the

Table 3 Observed asymmetry. Errors are dominated by statistics

$\{\ell, b\}$	$\mathcal{A} \times 10^3$
{264, 48}	-0.2 ± 1.0
{174, 0}	0.2 ± 1.0
{264, -42}	0.0 ± 0.9

asymmetry $\mathcal{A} = (\tau_S^+ - \tau_S^-)/(\tau_S^+ + \tau_S^-)$, we obtain the results of Table 3. Systematic uncertainties partly cancel for the asymmetries. Thus the systematic error is $\sim 0.2 \times 10^{-3}$. All asymmetries in Table 3 are consistent with zero. Using all KLOE data (about 2 fb^{-1}), the asymmetry in the direction of CMB anisotropy, is $(-0.13 \pm 0.40_{\text{stat}}) \times 10^{-3}$ also consistent with zero. Again systematic error is negligible.

Acknowledgements We thank the DAΦNE team for their efforts in maintaining low background running conditions and their collaboration during all data-taking. We want to thank our technical staff: G.F. Fortugno and F. Sborzacchi for their dedication in ensuring efficient operation of the KLOE computing facilities; M. Anelli for his continuous attention to the gas system and detector safety; A. Balla, M. Gatta, G. Corradi and G. Papalino for electronics maintenance; M. Santoni, G. Paoluzzi and R. Rosellini for general detector support; C. Piscitelli for his help during major maintenance periods. This work was supported in part by EURODAPHNE, contract FMRX-CT98-0169; by the German Federal Ministry of Education and Research (BMBF) contract 06-KA-957; by the German Research Foundation (DFG), ‘Emmy Noether Programme’, contracts DE839/1–4.

Open Access This article is distributed under the terms of the Creative Commons Attribution Noncommercial License which permits any noncommercial use, distribution, and reproduction in any medium, provided the original author(s) and source are credited.

References

1. F. Ambrosino et al. (KLOE Collaboration), Eur. Phys. J. C **48**, 767 (2006)
2. F. Ambrosino et al. (KLOE Collaboration), Phys. Lett. B **632**, 76 (2006)
3. F. Ambrosino et al. (KLOE Collaboration), Phys. Lett. B **632**, 43 (2006)
4. F. Ambrosino et al. (KLOE Collaboration), Phys. Lett. B **626**, 15 (2005)
5. F. Ambrosino et al. (KLOE Collaboration), J. High Energy Phys. **01**, 073 (2008)
6. F. Ambrosino et al. (KLOE Collaboration), Phys. Lett. B **666**, 305 (2008)
7. F. Ambrosino et al. (KLOE Collaboration), J. High Energy Phys. **04**, 073 (2008)
8. K. Nakamura et al. (Particle Data Group), J. Phys. G **37**, 075021 (2010)
9. F. Ambrosino et al. (KLOE Collaboration), Nucl. Instrum. Methods A **534**, 403 (2004)
10. F. Ambrosino et al. (KLOE Collaboration), J. High Energy Phys. **0712**, 073 (2007)
11. M. Adinolfi et al. (KLOE Collaboration), Nucl. Instrum. Methods A **488**, 51 (2002)
12. M. Adinolfi et al. (KLOE Collaboration), Nucl. Instrum. Methods A **482**, 364 (2002)

13. M. Adinolfi et al. (KLOE Collaboration), Nucl. Instrum. Methods A **492**, 134 (2002)
14. F. Bossi, E. De Lucia, J. Lee-Franzini, S. Miscetti, M. Palutan, KLOE Collaboration, Riv. Nuovo Cimento **31** (10), 531 (2008)
15. L. Bertanza et al., Z. Phys. C **73**, 629 (1997)
16. A. Lai et al., Phys. Lett. B **537**, 28 (2002)
17. A. Alavi-Harati et al., Phys. Rev. D **67**, 012005 (2003)
18. G. Hinshaw et al., Astrophys. J. Suppl. Ser. **180**, 225 (2008)